Star Formation with the Infrared Space Observatory
ASP Conference Series, Vol. 132, 1998
J. L. Yun, and R. Liseau, eds.

LWS Observations of Pre Main Sequence Objects

P. Saraceno, B. Nisini, M. Benedettini, C. Ceccarelli, A.M. Di Giorgio, T. Giannini, S. Molinari, L. Spinoglio

Istituto di Fisica dello Spazio Interplanetario, CNR - Frascati, Italy

P.E. Clegg, J.C. Correia, M.J. Griffin, S.J. Leeks, G.J. White

Queen Mary & Westfield College, Mile End Road, London E1 4NS, UK

E. Caux

CESR, BP4346, F-31028 Toulouse Cedex 04, France

D. Lorenzetti

Osservatorio di Roma, I-00040 Monteporzio, Italy

E. Tommasi

ISO SOC, P.O.box 50727, 28080 Vilspa Spain

R. Liseau

Stockholm Observatory, S-133 36 - Saltsjobaden, Sweden

H. A. Smith

Smithsonian Center for Astrophysics, MA 02138 Cambridge, USA

Abstract.

We review the first results of a 45-190 μm spectroscopic study of a sample of Class 0, Class I, Class II (Herbig Ae/Be) and Herbig-Haro objects. In the observed Class 0, Class I and HH objects J shocks can account for the [OI] observed intensity, while for Ae/Be stars the [OI] emission is mainly due to the presence of photodissociation region. For some Class 0 and Class I sources, high-J CO transitions are the dominant FIR coolants, indicating the additional presence of C shocks. In these sources the H_2O cooling is significantly less than that predicted by models. Finally, evidence is seen for [OI] 63μm self-absorption in all the Class I and the Class II objects of the sample.

1. The LWS sample of preMS objects

The main objective of the ISO-LWS pre Main Sequence (preMS) programme is the study of preMS stellar evolution using 3-200μm spectrophotometric observations of a sample of Class 0 (André et al. 1993), Class I and Class II (Lada & Wilking 1984) sources. The objects of the "LWS sample" were selected for having relatively strong submillimeter continuum emission and (with few exceptions among Class II sources) for being associated with molecular outflows.

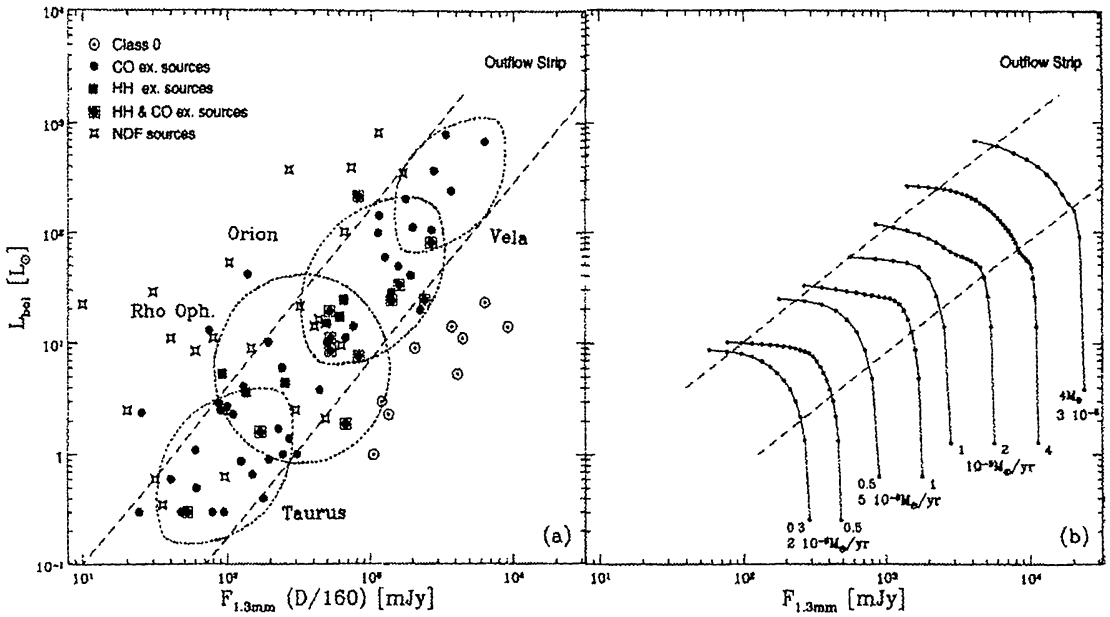

Figure 1. a) the L_{bol} *vs* F^D_{mm} diagram; b) the computed tracks

Additional submillimeter line (CO) and continuum observations were made at the SEST (Swedish ESO Submm Telescope) and JCMT (James Clerck Maxwell Telescope). The results of this work are given in Saraceno et al. (1995, 1996a), where the ISO-LWS targets are presented in a L_{bol} *vs* F^D_{mm} diagram (Fig.1a), being F^D_{mm} is the 1.3 mm flux scaled at the distance D ($\simeq$ to L_{mm}).

This diagram has been found to be a good diagnostic tool to trace the preMS evolution: Class I sources associated with Herbig-Haro objects (HH) or molecular outflows show a correlation between L_{bol} and F^D_{mm} and lie in the region called "Outflow Strip", while Class 0 sources lie on the right of this region and Class I without associated outflow lie mostly on the left side. Since evolution proceeds from high to low values of the millimeter flux ($\propto$ circumstellar material), Class 0 sources are the youngest objects while sources without outflow are the most evolved.

These results are consistent with the evolutionary tracks shown in Fig.1b, where progenitor clumps of different masses and accretion rates are considered. Each point on the track corresponds to constant time steps; the concentration of

points in the upper part of the tracks traces a theoretical "outflow strip", which broadly corresponds to the deuterium burning phase.

Fig.1a also shows that sources belonging to different clouds are segregated into well defined areas of the "outflow strip"; moving along the strip, the circumstellar mass ($\propto F^D_{mm}$), the mass of the formed star ($\propto L_{bol}$) and the accretion rate all increase. The LWS sample is therefore representative of low to intermediate mass star formation in nearby clouds. Class I sources lacking outflows were rejected because they seem to be evolved objects obscured by foreground material.

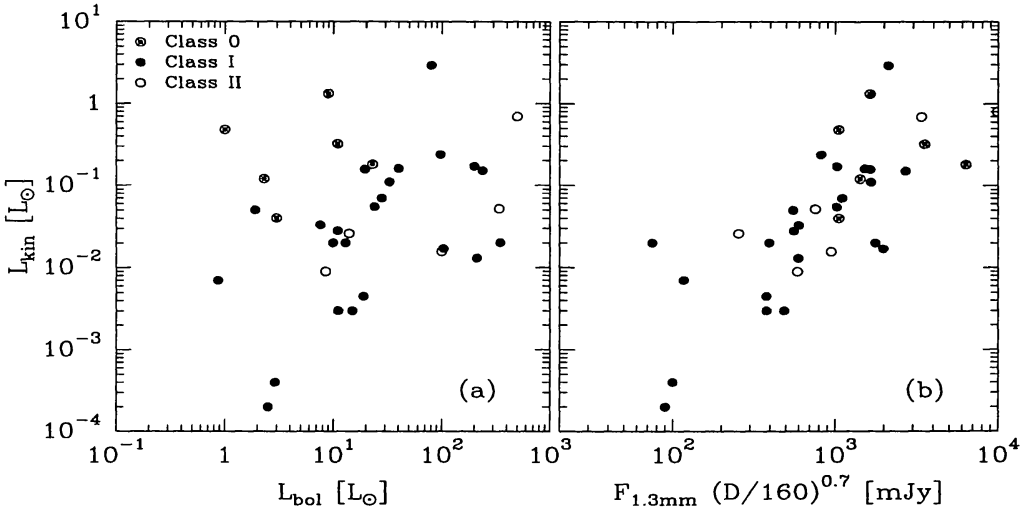

Figure 2. L_{kin} *vs* L_{bol} and L_{kin} *vs* F^D_{mm} diagrams.

In Fig.2 a subsample of the LWS sources is presented in the L_{kin} *vs* L_{bol} and L_{kin} *vs* F^D_{mm} diagrams, where L_{kin} is the kinetic luminosity. For all the considered categories (in particular for Class 0 and Class I sources) L_{kin} appears to be better correlated with the disk-envelope system ($\propto F^D_{mm}$) rather than with the luminosity of the central source ($\propto M_*$), showing that accretion, circumstellar mass and outflow are connected together in all phases of the star formation.

2. The LWS Observations

All sources of the LWS program are observed with the LWS in the grating mode ($R \sim 200$, $FOV \sim 80$", Clegg et al. 1996) and some of them with the SWS to obtain low resolution spectra in the 3-200 μm range. Additional FP observations are foreseen as "follow up" of the grating observations.

The results available at the time of this conference are still preliminary, for the following reasons: i) large part of the program has still to be carried out because most of the LWS sources are in the regions of Perseus, Taurus and Orion (Fig.1a), only visible since August 1997; ii) several spectra are still affected by strong fringes (a problem not fully solved); iii) Fabry-Perot observations have not been carried out and we do not have information on the dynamics, essential

to discriminate among the different emitting regions; iv) the reduction of our SWS spectra is at a preliminary stage.

Despite this, the present volume contains 11 contributions dealing with the available data of the preMS-LWS program. Here we will try to outline some general results for the different categories of objects.

3. PDR and Shocks

The FIR line emission of young stellar objects is mainly originated from two physical processes: the excitation from photoionised and photodissociated (PDR) regions (Wolfire et al. 1990) and the shock excitation produced by the interaction of supersonic winds with the ambient medium. Depending on wind velocity, magnetic field and ion density, two kinds of shocks with different FIR spectra are predicted from models: i) high velocity dissociative "J" shocks (e.g. Hollenbach & McKee 1989), in which temperature, density and velocity have a discontinuous jump ("J") on the shock front, molecules are dissociated and atomic lines are the dominant coolants; ii) low velocity non-dissociative "C" shocks (e.g. Kaufman & Neufeld 1996, Draine et al. 1983) in which the Alfven velocity is larger than the shock velocity and the magnetic field transmits energy faster than the shock velocity; in this case temperature, density and velocity have a continuous ("C") variation and molecules are the dominant coolants.

In the LWS range there are several lines that are crucial to discriminate between PDR and shock excitation and to understand the shock physics.

Source	Class	L_{bol}	$L_{[OI]}$	L_{CO}	L_{H_2O}	L_{OH}	L_{lines}	$\frac{L_{mol}}{L_{[OI]}}$	$\frac{L_{lines}}{L_{bol}}$
B335 FIR	0	3	0.002	0.004	...	...	0.006	2	2 E-3
IRAS16293	0	27	0.005	0.04	0.003	0.003	0.05	9.2	1.8 E-3
IC1396 N	I	235	0.1	0.63	0.17	...	0.9	8	3.8 E-3
HH54B	HH	-	0.0026	0.01	0.002	0.001	0.039	0.5	
R CrA	II	132	0.038	0.03	...	0.01	0.078	1.05	5.9 E-4
IRAS12496	II	50	0.005	0.008	...	...	0.013	1.6	2.6 E-4

Table 1: Line cooling; the luminosities are expressed in $L_\odot$

Table 1 lists all the objects with detected molecular lines for which it was possible to compute the cooling by means of a LVG model (Nisini et al. this volume). Only one HH, out of a sample of 17 (Liseau et al 1997) and three Herbig Ae/Be stars out of a group of 10 (Lorenzetti et al this volume) showed molecular lines. For the HHs and Ae/Be stars the table is therefore representative of the relevance of molecular lines in these objects. On the contrary for Class 0 and Class I sources the table is not statistically representative: we observed 15 Class 0 and low luminosity Class I sources and in nearly half of them we detected molecular lines. However, only for the three objects listed in the table it was possible, at the present level of data analysis, to compute the line cooling. In the 8th column of the table, the ratio between the total molecular line and [OI] 63μm

line luminosities is given: we note that the molecular line cooling dominates the Class 0 and Class I sources while for the Ae/Be stars the two coolings are similar.

Since atomic oxygen is the main coolant in dissociative "J" shocks, Hollenbach (1985) suggested that the mass loss rate should be proportional to the [OI] 63μm line luminosity through the simple relationship:

$$\dot{M}_{wind} = 10^{-4}(L([OI]63\mu m)/L_{\odot} \quad [\dot{M}_{\odot} yr^{-1}] \tag{1}$$

Moreover, assuming that $\dot{M}_{wind}$ remains relatively constant during the outflow life and accepting the common assumption that the momentum is conserved in the wind-molecular flow interaction, $\dot{M}_{wind}$ can also be estimated from:

$$\dot{M}_{wind} V_{wind} = \dot{M}_{CO} V_{CO} \tag{2}$$

For optically and NIR visible sources V_{wind} is obtained from Hα or NIR observations, for embedded objects a typical value of 100 km s^{-1} is assumed. M_{CO} and V_{CO} are estimated from millimeter CO maps.

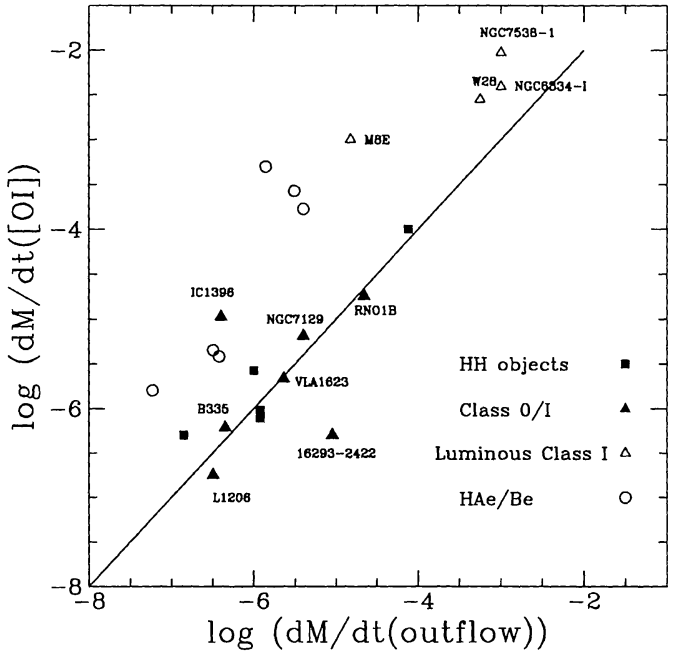

Figure 3. Stellar mass loss rates estimated from the [OI] 63μm line and millimeter CO observations.

All the observed sources for which we found literature data for $\dot{M}_{CO}$ are reported in Fig.3, where the mass loss rate derived from the [OI] intensity is reported versus the rate obtained from the molecular outflow. Data for 5 HH have been taken from Liseau et al. (1997) and for 6 Ae/Be stars from Lorenzetti

et al. in this volume. In addition we report 4 low luminosity Class I, 4 high luminosity Class I and 3 Class 0 sources whose names are given in the figure.

The solid line represents equal values of the two mass loss determinations; the [OI] emission of objects on the line is therefore likely to come from dissociative "J" shocks. For a source to be above the line is an indication of [OI] emission in excess of that predicted by "J" shock models, probably due to the presence of different excitation mechanisms (HII regions, PDR). The sources below the line have an [OI] emission too low to be emitted in dissociative "J" shocks and are probably related to "C" shocks or weak PDRs. The objects of our program group in different regions of Fig.3. Above the line we find:

- **Herbig Ae/Be stars:** as discussed by Lorenzetti et al. in this volume, the [OI] emission of these objects is accounted for by PDR models, in agreement with their position in Fig.3. Some of them also show molecular emission consistent with "C" shock models. The luminosity of the FIR lines ranges between 2 and 6 $\cdot 10^{-4}$ L_{bol} (last column in Table 1), about 10 times less than the value obtained for Class 0/I sources.

- **High luminosity Class I objects,** $L > 10^4 L_\odot$**:** these sources are surrounded by relatively large ionised and PDR regions that explain both the relative lack of molecular lines and the presence of intermediate ionisation lines, such as [NIII], [OIII] (Leeks S.J. et al. in preparation).

- **IC1396N:** this is a low luminosity Class I source at the edge of an extended HII region excited by an O6 star (see Molinari et al., this volume and Saraceno et al. 1996b). It has a very peculiar spectrum showing both the molecular lines typical of low luminosity Class I sources (observed only "on source") and the atomic lines of bright objects ([OI], [NII],[NIII], [OIII]) observed also "off source", due to the UV photons of the O6 stars. The increased [OI] emission moves it above the solid line in Fig.3.

Below the line we find **IRAS 16293** a Class 0 source (see Ceccarelli et al., this volume) with a [OI] emission weaker than that expected from the millimeter data. For this object $L_{CO} \sim 8 L_{[OI]}$ (Table 1) indicating that non-dissociative "C" shock excitation is the dominant physical process, and therefore the [OI] intensity is not expected to be proportional to the mass loss rate.

On the line, we find the following sources, for which dissociative "J" shocks should play an important role:

- **The Herbig-Haro objects:** in Liseau et al. (1997) a review of our results on 17 HHs taken in 7 different regions is reported. In all HHs the [OI] 63μm line is the dominant FIR coolant with an emission spatially associated with the HH objects. On 7 objects the [OI] 145μm line has also been detected. Finally, only in HH54 (Liseau et al. 1966) we detect molecular lines (Table I) which agree with both "J" and "C" shock models (see in the following). This scenario indicates that dissociative "J" shocks are the prominent physical process for HHs excitation. We also notice that HHs ("J" shocks) are the only sources in which we have evidence of shocked gas in beams that do not contain the flow exciting source.

- **Class 0 and low luminosity Class I sources:** the few objects for which molecular line cooling has been computed (Table 1) show $L_{CO} > L_{[OI]}$ suggesting that in contrast to HH objects, both "J" and "C" shocks play an important role (see Nisini et al. and Ceccarelli et al. in this volume). A review of models considering the simultaneous presence of both "C" and "J" shocks can be found in Hollenbach (1997). Here we point out the importance of FP observations of the [OI] 63 μm (tracer of "J" shocks) and of CO and H_2O lines (a tracers of "C" shocks) in order to understand if "J" and "C" shocks come from the same regions (= same velocity).

Finally we emphasize that the correlation between the two M_{wind} determinations, which HH, Class 0 and low luminosity Class I sources show in Fig.3, is particularly good in spite of the uncertainty in relationship (2) due to the determination of CO opacity and flow angle. The different dependence with distance of the [OI] data (point-like in the LWS beam) and of the millimeter CO data (extended in the mm telescopes beam) does not have a strong influence, because the objects on the line are at about the same distance (within a factor 2).

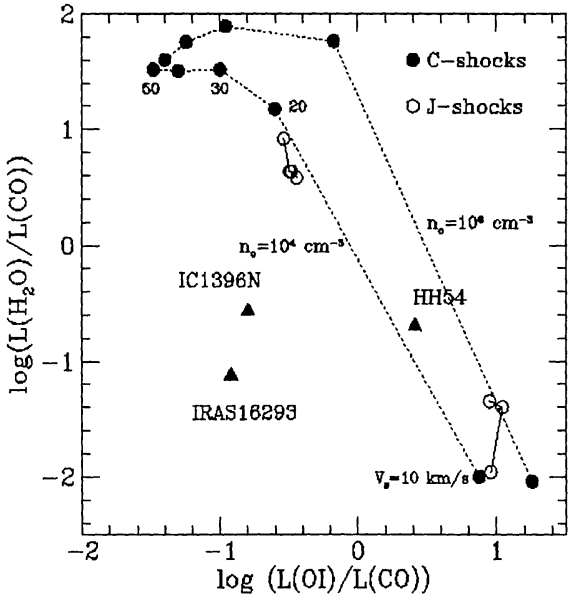

Figure 4. Line cooling predicted by "J" and "C" shock models

3.1. Dissociative shocks and H_2O abundance

Non dissociative shocks were expected to be "prodigious sources of far infrared water emission" (M. Kaufman and D. Neufeld, 1996) because H_2O forms very efficiently at temperatures above 400 K, which is typical of post-shock gas. Indeed, post-shock water abundances in excess of 10^{-5} are predicted by models (e.g. Draine et al 1983), with all the O not locked in CO transformed in water.

Water has been detected in several objects, but up to now only for three of them, namely HH54 (Liseau et al.1996), IC1396N (Molinari et al. this volume) and IRAS 16293 (Ceccarelli et. al. this volume) it is possible to compute the line cooling as reported in Table 1. A comparison with L_{CO} shows that H_2O plays only a minor role in the thermodynamic balance in any of these objects.

This discrepancy between models and observations can be better seen from Fig.4 where a L_{H_2O}/L_{CO} vs $L_{[OI]}/L_{CO}$ diagram is plotted along with the predictions of "C" and "J" shock models. In "C" shocks the threshold temperature for H_2O formation is reached at velocities $>$ 20 km s^{-1} where, in the figure, there is a jump of 3 orders of magnitude in the H_2O emission. Similar curves are presented for "J" shocks (open dots) for velocities of 30 and 50 km s^{-1} and pre-shock densities of 10^4 (bottom) and $10^6 cm^{-3}$ (top).

If we compare model results with observations, we notice that, while HH54 agrees with both "C" and "J" shocks, IC1396N and IRAS 16293 lie outside the regions covered by models. For IC1396N the situation is even worse because (Fig.3) most of the [OI] results from PDR emission and consequently its position in the diagram should move to the left. The observed discrepancy indicates a lack of water production in "C" type shocks; a possible explanation could be that in "C" shocks a large amount of oxygen is not available in atomic form but remains locked into grains or in O_2 and does not form water. (see also Ceccarelli et al in this volume).

4. [OI] self-absorption

In the previous paragraph we have seen that the [OI] 63μm line is a good diagnostic tool for discriminating between PDRs and shock excitation. But when we tried to use the ratio R = [OI] 63μm/[OI] 145μm in the diagnostic diagrams, as suggested by several authors (i.e. Wolfire et.al 1990, Hollenbach & Mc Kee 1989, Keenan & Colon 1994), we found values of R too low for being consistent with models. For Class I sources the values of R range between 4 and 12, while for Class II sources this ratio is between 7 and 14; only in very extreme cases the models can reach values of 10-12, but not lower. Such low values could be explained (Tielens & Hollenbach, 1985, Fig.2) by the emission of a relatively high column density of cold (<100K) atomic oxygen, in contradiction with the evidence of the warm shocked gas given in the previous paragraph.

The only other possibility to explain such low values of R is to assume that the [OI] 63μm is self-absorbed by a much cooler gas on the line of sight, as observed toward several galactic (i.e. Poglitsch A. et al. 1996, Baluteau et al. 1997) and extragalactic objects (i.e. Fischer et al 1997).

To check this hypothesis, since the data are still affected by systematic errors, due in particular to the defringing process, we adopted a statistical approach, looking at the distribution of the ratio R among the different categories of objects. We separately consider Class I sources, Class II sources, HHs, and the "off source" pointings of Class I and Class II sources. To these 5 groups we added a group of ultracompact HII regions (UCHII; P. Cox, private communication) and Planetary Nebulae (PN; M. Barlow private communication), having a total of 7 groups of objects which are plotted as the series of histograms in Fig.5. On the x-axis, the ratio R is reported. The total number N of objects

considered in each category is given on the right of each histogram together with the average ratio $\bar{R}$. The histograms are ordered following increasing values of $\bar{R}$ from the bottom to the top.

A very simple analysis of the histograms shows that the objects have a relatively low dispersion and are sufficiently numerous to make the results statistically significant. The ordering of the categories shows that an increase of the $\bar{R}$ value corresponds to a decrease of the circumstellar mass. The lowest ratio is observed in UCHII regions, which are located in star forming regions more massive than those where the Class I sources are located. Then we have Class I sources and their "off source" (which, being taken close to the "on source", are still inside the parental cloud), Class II sources and their "off sources", HH objects and finally the PN which show the largest dispersion probably due to intrinsic differences in the circumstellar masses. This result suggests that the absorption is mainly due to colder gas, still associated to the source, and not to gas along the line of sight, as also shown by the "off source" pointings that have values similar but always higher than those "on source".

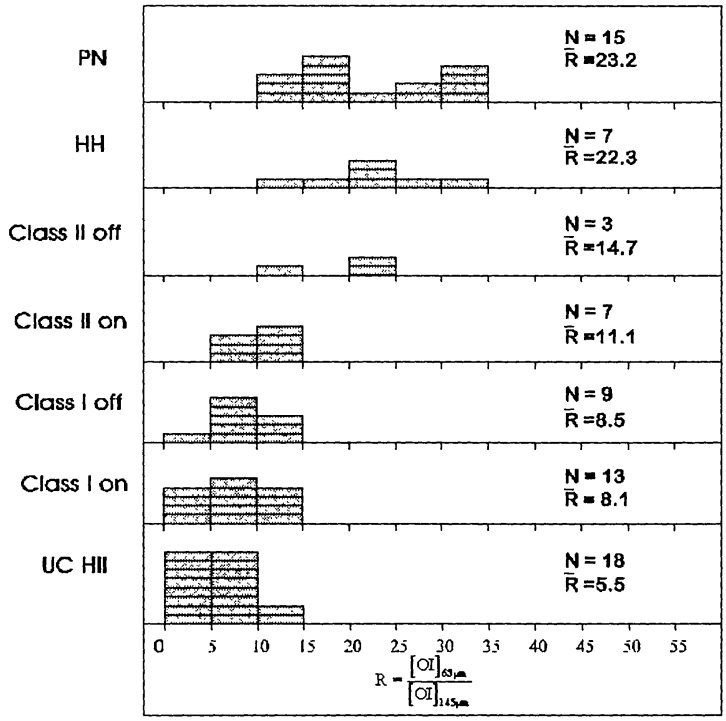

Figure 5. The distribution of the ratio of $\frac{[OI]63\mu m}{[OI]145\mu m}$ among different categories of objects.

In order to have the [OI] 63μm self-absorption necessary to reach the ratio R foreseen from models, it would be sufficient to have an optical depth $\tau \sim 1$. Optical depths of this order are expected in star forming regions; if we write the column density as N[OI] $\sim 2\ 10^{17}\ \Delta V \tau\ cm^{-2}$ (Poglitsh et al. 1996), where

ΔV$\sim$ 1 - 3 Km/s is the velocity dispersion of the cold absorbing gas, for $\tau = 1$ we find N[OI] $\sim$ 2 - 6 10^{17} cm^{-2}.

If only 1/100 of the cosmic oxygen is in atomic form we obtain that, to have the observed self-absorption, a column density N[H_2] $\sim$ 2 - 6 10^{22} cm^{-2} is required, a value easily found in the environment of our sources (e.g. for IC1396N we find N[H_2] $> 10^{23}$ cm^{-2}, Saraceno et al. 1996b).

4.1. Conclusions

We give the first review of the results obtained with the LWS programme for the study of preMS evolution. We find that the observed:

- luminous objects (Class I and Class II sources) are dominated by photoionization and PDR emission;
- Herbig Haro objects show the emission expected from dissociative shocks;
- several Class 0 and low luminosity Class I sources show evidence for the presence of both dissociative and non-dissociative shocks. In some sources the molecular lines are the major FIR coolant;
- H_2O cooling seems to be lower than the model predictions;
- Class I and Class II sources show evidence of [OI] 63μm self-absorption.

Acknowledgments. The authors thank M. Barlow and P. Cox for providing the [OI] data for the Planetary Nebulae and Ultracompact HII regions, Mike Luhman for the several useful discussions and the whole LWS consortium which made these observations possible. S.J.Leeks is pleased to acknowledge receipt of a PPARC award. ISO is an ESA project funded by ESA member states.

References

André P., Ward-Thompson D., Bersony M. 1993, ApJ 406,122
Baluteau J.P. et al. 1997, A&A 322,L33
Clegg P.E. et al. 1996, A&A 315,L38
Draine B.T., Roberge, W.G. and Dalgarno 1983, ApJ 264,485
Fischer J. et al. 1997, XVIIth Moriond Astronomy Meeting, in press
Hollenbach D. 1985, Icarus, 61,40
Hollenbach D., McKee C. 1989, ApJ 342,306
Hollenbach D., 1997, IAU Symposium N.182,181
Kaufman M.J., Neufeld D.A. 1996, ApJ 456,611
Keenan F.P., Colon E.S. and Rubin R.H. 1994, ApJ 434,811
Lada C. J., Wilking, B.A. 1984, ApJ, 287,610
Liseau R. et al. 1997, IAU Symposium N.182,111
Liseau R. et al. 1996, A&A, 315,L181
Poglitsch A. et al. 1996, ApJ, 462,L43
Saraceno P. et al. 1995, ESO Workshop "The Role of Dust in the Formation of Stars", Garching 11-14 Sept 1995
Saraceno P., André P., Ceccarelli C., Griffin M., Molinari S. 1996a, A&A, 309,827.
Saraceno P. et al. 1996b, A&A 315, L293
Tielens A.G.G.M., Hollenbach D. 1985, ApJ 291,722
Wolfire M.G., Tielens A.G.G.M., Hollenbach D. 1990, ApJ 358,116